JOURNAL OF CATALYSIS 79, 396–409 (1983)

Pt–Mo Bimetallic Catalysts Supported on Y-Zeolite

I. Characterization of the Catalysts

T. M. TRI, J.-P. CANDY, P. GALLEZOT,[1] J. MASSARDIER, M. PRIMET, J. C. VÉDRINE, AND B. IMELIK

Institut de Recherches sur la Catalyse, C.N.R.S., 2 Avenue Albert Einstein, 69626 Villeurbanne Cédex, France

Received April 7, 1982; revised July 27, 1982

Bimetallic PtMoY catalysts have been prepared by adsorption and decomposition of $Mo(CO)_6$ in a Y-type zeolite containing 10-Å Pt particles trapped in the zeolite cages. Part of the Mo atoms are deposited onto the Pt particles which produces a weak increase of the particle size measured by CTEM and STEM and a progressive decrease of the amount of H_2 or CO chemisorbed on platinum. At high Mo contents these chemisorptive properties are completely masked. It was checked by XPS, X-ray absorption edge spectroscopy, and ir spectroscopy with CO and NO as probe molecules that the Pt particles are initially electron deficient but the electronic structure becomes similar to that of bulk platinum once the Mo atoms were added. This is probably because the Pt atoms are then shielded from the electron acceptor sites of the support. The Mo atoms bonded to Pt are probably in a low valence state, but there is a fraction of Mo not bonded to Pt, especially in the zeolite outer layers of Mo-rich samples, which is oxidized to Mo^{IV}–Mo^{VI} by oxido-reduction reactions with the zeolite protons.

INTRODUCTION

The states of the two components in bimetallic catalysts are often poorly characterized and it is therefore difficult to settle how one of the components affects the catalytic properties of the other. Progress can be achieved by studying precisely built bimetallic systems with smaller particle sizes than those obtained by reducing mixtures of metal oxides or salts. In that respect, the decomposition on supports of heteropolynuclear, molecular clusters of known structure, in which the transition metal atoms are already linked via metal–metal bonds, could become a valuable preparative method. Meanwhile, the method used by Yermakov and Kuznetsov (*1*) to anchor bimetallic clusters on supports appears suitable to prepare well-defined materials. $Pt–Mo/SiO_2$ catalysts have thus been prepared by reduction of Mo $(\pi\text{-}C_3H_5)_4$ complexes yielding low-valent Mo atoms grafted on silica which act as anchoring sites for the Pt atoms coming from the reduction of $Pt(\pi\text{-}C_4H_7)_2$ complexes. In this work the PtMo catalyst has been prepared by adding molybdenum from the decomposition of $Mo(CO)_6$ onto 10-Å platinum particles trapped in Y-type zeolite, a system which has been studied thoroughly in previous work (*2–8*). The PtMo bimetallic catalyst has been studied by several techniques to characterize the dispersion and the electronic structure of the two components. The study of the adsorption and catalytic properties of the PtMoY zeolites will be reported in a subsequent paper as Part II.

EXPERIMENTAL

1. Preparation of the catalysts. The NaY Linde SK40 zeolite ($Na_{56}Al_{56}Si_{136}O_{384}$) has been exchanged in ammonia solution of $PtCl_2$ as previously described (*2*). The zeolite was washed with ammonia and water

[1] To whom correspondence should be addressed.

0021-9517/83/020396-14$03.00/0

until the wash waters were free from Cl^- ions. The unit cell compositions of the calcined zeolites were determined by chemical analysis of Pt^{2+} and Na^+. The exchanged zeolites (1 g batch) have been heated under flowing oxygen from 300 to 650 K at 0.5 K min^{-1}, then reduced at 600 K under 400 Torr (1 Torr = 133.3 Pa) of H_2 pressure. Under these conditions, Pt particles of ca. 10 Å diameter are formed in the zeolite supercages (*2*). The PtMoY zeolites were prepared from the PtY zeolites by adsorption and decomposition of $Mo(CO)_6$ vapor. The PtY zeolites were reactivated under hydrogen and then outgassed at 600 K in the first branch of a glass cell. The $Mo(CO)_6$ powder, in suitable amount to obtain the required loading, was introduced in the second branch which was evacuated at 300 K. The two branches were then connected via a grease-free stopcock and the cell was placed in an oven at 340 K for 12 h. It was checked by gravimetry that the zeolites took up the whole amount of the carbonyl. The Mo-loaded zeolites were then heated at 600 K under 300 Torr of H_2 pressure to decompose the $Mo(CO)_6$ molecules. Finally the PtMoY zeolites were evacuated at 600 K. In two cases, the PtY zeolites were treated at 900 K in vacuum in order to dehydroxylate the zeolite framework before adsorption and decomposition of $Mo(CO)_6$. The various samples thus obtained are described in Table 1.

2. Methods. The zeolites were examined both with a high-resolution conventional electron microscope, CTEM (Jeol-JEM 100 CX) and with a scanning transmission electron microscope STEM (Vacuum Generators, HB5) which provides analytical capability over a specimen projected area as small as 400 $Å^2$. The CTEM and STEM investigations were performed on carbon film replica and on ultramicrotome cuts (100–800 Å thick) of the zeolite crystals.

The adsorption measurements of H_2 and O_2 were carried out volumetrically in a grease-free vacuum and gas line equipped with a turbomolecular pump. The pressure in the adsorption cell was measured with a Texas Instruments gauge. The amount of gas desorbed from the samples can be evaluated from the increase of pressure measured with a McLeod gauge in the reservoir

TABLE 1

Nomenclature, Composition, and Treatments

Samples	Unit cell composition	Pt (wt%)	Mo (wt%)	Pt/(Pt + Mo) (atoms)	Treatments
PtY,I	$Pt_{7.6}Na_{30.9}H_{9.9}Y$	10.9	0	1	650 K in O_2, 600 K in H_2 (400 Torr)
PtY,II	$Pt_{3.2}Na_{29.5}H_{20.1}Y$	4.8	0	1	650 K in O_2, 600 K in H_2 (400 Torr)
PtMoY,I	$Pt_{7.6}Na_{30.9}Mo_{1.7}Y$	10.9	1.2	0.82	PtY,I evacuated at 600 K, $Mo(CO)_6$ adsorbed at 340 K, decomposed at 600 K under H_2
PtMoY,II	$Pt_{7.6}Na_{30.9}Mo_{5.0}Y$	10.6	3.4	0.61	PtY,I evacuated at 600 K, $Mo(CO)_6$ adsorbed at 340 K, decomposed at 600 K under H_2
PtMoY,III	$Pt_{7.6}Na_{30.9}Mo_{8.3}Y$	10.4	5.6	0.48	PtY,I evacuated at 600 K, $Mo(CO)_6$ adsorbed at 340 K, decomposed at 600 K under H_2
PtMoY,IV	$Pt_{7.6}Na_{30.9}Mo_{12.2}Y$	10.1	8.0	0.38	PtY,I evacuated at 600 K, $Mo(CO)_6$ adsorbed at 340 K, decomposed at 600 K under H_2
PtMoY,V	$Pt_{3.2}Na_{29.5}Mo_{8.0}Y$	4.5	5.5	0.29	Prepared as PtMoY,I, from PtY,II
PtMoY,VI	$Pt_{0.4}Mo_8Na_{55}Y$	0.5	5.6	0.04	Prepared as PtMoY,I, from $Pt_{0.4}Na_{55}Y$
PtMoY,VII	$Pt_{6.9}Mo_{4.8}Na_{19.6}Y$	9.4	3.4	0.58	Zeolite $Pt_{6.9}Na_{19.6}H_{22.6}Y$ evacuated at 873 K, $Mo(CO)_6$ adsorption and decomposition as for PtMoY,I.
PtMoY,VIII	$Pt_{6.9}Mo_{7.2}Na_{19.6}Y$	9.2	5.0	0.48	Zeolite $Pt_{6.9}Na_{19.6}H_{22.6}Y$ evacuated at 873 K, $Mo(CO)_6$ adsorption and decomposition as for PtMoY,I.
MoNaY	$Mo_8Na_{55}Y$			0	Zeolite NaY treated as PtY,I

of primary vacuum isolated from the manifold pump. All the dead volumes were calibrated with He. The catalysts were evacuated at 673 K prior to H_2 and O_2 adsorption. Programmed thermodesorption measurements were also carried out; the samples precovered with H_2 were heated at 40 K min^{-1} under high vacuum maintained with a high velocity pumping device. The H_2 desorbed from the sample was detected with a quadrupole mass spectrometer.

The X-ray absorption spectra at the Pt L III absorption edge were taken with synchrotron radiation with a X-ray spectrometer at the LURE facility (Orsay, France). Wafers of zeolite were treated and maintained during recording under controlled atmosphere in a glass cell equipped with beryllium windows.

The photoelectron emission spectra were taken with a Vacuum Generators ESCA 3 spectrometer. The zeolites, set on a grid, were reduced *in situ* at 573 K under a low H_2 pressure (1 Torr).

The ir spectra were recorded with a Perkin Elmer 580 instrument. The zeolites were pressed into 20-mg wafers and treated in a glass cell equipped with ir transparent windows.

RESULTS

1. Electron Microscopy Investigation

Examination of replica and ultramicrotome cuts by CTEM indicates that the platinum particles are very homogeneously scattered throughout the zeolite bulk in the PtY,I and PtY,II samples as well as in all the Mo-loaded samples. This was corroborated by the STEM investigation. The analysis of platinum by the built-in X-ray spectrometer carried out on 100 nm^2 projected area of zeolite slabs demonstrates the uniform distribution of platinum.

In contrast, the molybdenum formed by $Mo(CO)_6$ decomposition is not evenly distributed, especially in the Mo-rich and Pt-poor samples. Thus clusters of 10- to 20-nm Mo particles were observed on the external surface of a Pt-free MoNaY and in PtMoY-VI samples. In all the other samples such particles were not observed but the microanalysis by STEM showed that the Pt/Mo ratio varies from crystal to crystal and within a given crystal from the outer layers to the core. Inhomogeneity in Mo distribution is marked mainly in samples where Pt/(Pt + Mo) is smaller than 0.5. Analyses were also carried out on a smaller specimen area in an attempt to analyze the composition of a single particle. Unfortunately the analyzer was not sensitive enough to detect Pt or Mo because the particles contain too few atoms.

Particle sizes on PtY and PtMoY zeolites were measured by counting several hundreds of particles on different transmission photographs taken on ultramicrotome cuts. Figure 1 gives the distribution $\Sigma n_i d_i$ of the particle diameters for PtY,I and PtMoY,III. There is a shift of the distribution toward larger particle sizes as Mo atoms were loaded onto PtY,I. The average particle diameter $\Sigma n_i d_i / \Sigma n_i$ is 0.95 nm in PtY,I and

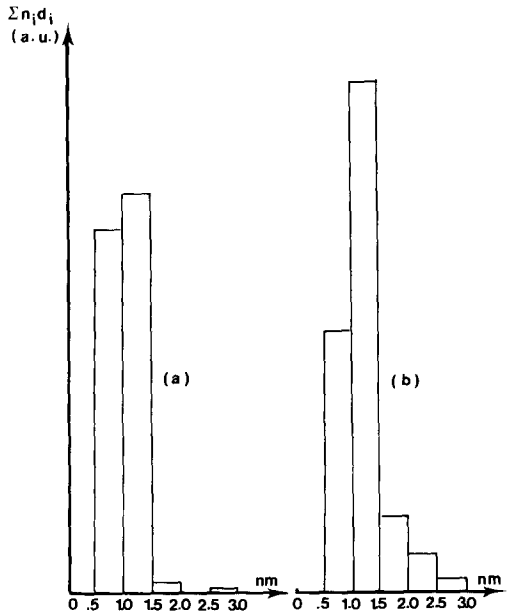

FIG. 1. Particle size distribution measured by TEM on ultramicrotome cuts of zeolite crystals; (a) PtY,I; (b) PtMoY,III.

1.06 nm on PtMoY,III. Measurements on other samples indicate that most of the particles are within 1 ± 0.3 nm in PtY zeolites and within 1.3 ± 0.3 nm in PtMoY zeolites.

2. *Adsorption and Desorption Measurements of H_2 and O_2*

The amounts of H_2 adsorbed and desorbed from the zeolite as measured volumetrically are given in Table 2. The $Q_1(H_2)$ amounts were taken up at 300 K under 50 Torr of H_2 whereas the $Q_2(H_2)$ amounts were measured after heating the zeolite from 300 to 573 K and then cooling down to 300 K under 50 torr of H_2. These amounts correspond entirely to a chemisorption uptake (rather than to a reduction process) since $D_1(H_2)$ and $D_2(H_2)$, the volumes desorbed at 673 K, are equal to $Q_1(H_2)$ and $Q_2(H_2)$ respectively. Since the hydrogen chemisorption decreases when Mo is progressively added it was assumed that the Mo species do not adsorb hydrogen. The H/Pt ratios are given in column 4 of Table 2. The additional amount of H_2 taken up at high temperature $\Delta Q = Q_2(H_2) - Q_1(H_2)$ cannot be correlated with the Pt or the Mo content of the zeolite but rather to the total amount of Pt + Mo present since the ΔQ/(Pt + Mo) ratio (column 9, Table 2) is almost constant. The values of the hydrogen uptake at 300 K, $\Delta Q_1(H_2)$, have been plotted (after normalization at unity for PtY,I) as a function of the Pt/(Pt + Mo) ratio in Fig. 2.

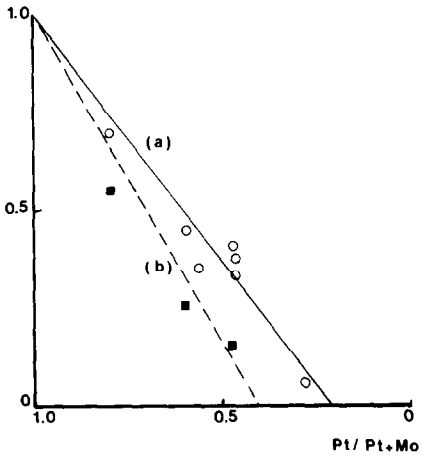

FIG. 2. Plot of $Q_1(H_2)$, hydrogen uptake at 300 K (normalized at 1 for PtY,I) vs Pt/(Pt + Mo). (b) Plot of the optical density of the ν_{CO} band at 2090–2067 cm^{-1} (normalized at 1 for PtY,I) vs Pt/(Pt + Mo).

TABLE 2

Volumetric Measurements of Adsorption and Desorption of Hydrogen[a]

Samples	Pt/(Pt + Mo)	$Q_1(H_2)$[b]	H/Pt[c]	$D_1(H_2)$[d]	$Q_2(H_2)$[e]	$D_2(H_2)$[f]	ΔQ[g]	ΔQ(Mo + Pt)[h]
PtY,I	1	6.1	0.96	6.2	7.2	7.2	1.1	1967
PtMoY,I	0.82	4.2	0.68	4.2	5.2	5.1	1.0	1484
PtMoY,II	0.61	2.7	0.45					
PtMoY,III	0.48	2.5	0.41		4.3		1.8	1612
PtMoY,IV	0.48	2.3	0.39	2.4	3.7	3.7	1.4	1253
PtMoY,V	0.29	0.36	0.14					
PtMoY,VI	0.04	0.08	0.03	0.08	0.81	0.8	0.73	1219
PtMoY,VII	0.58	2.1	0.40					
PtMoY,VIII	0.48	2.0	0.37					

[a] Amounts of H_2 adsorbed or desorbed are given in cm^3 of H_2 (NTP) g^{-1} of catalyst.
[b] $Q_1(H_2)$, uptake of H_2 at 300 K under 50 Torr of H_2 on catalyst outgassed at 673 K.
[c] H/Pt assuming that H_2 is adsorbed on Pt only.
[d] $D_1(H_2)$, amount of H_2 desorbed at 673 K under vacuum after H_2 adsorption at 300 K.
[e] $Q_2(H_2)$, uptake of H_2 under 50 Torr of H_2 after heating from 300 to 573 K and cooling from 573 to 300 K.
[f] $D_2(H_2)$, amount of H_2 desorbed at 673 K under vacuum after H_2 adsorption at 300–573–300 K.
[g] ΔQ, difference between the H_2 uptake at 573 and 300 K, $Q_2(H_2) - Q_1(H_2)$.
[h] ΔQ(Mo+ Pt), ΔQ per total metal atoms.

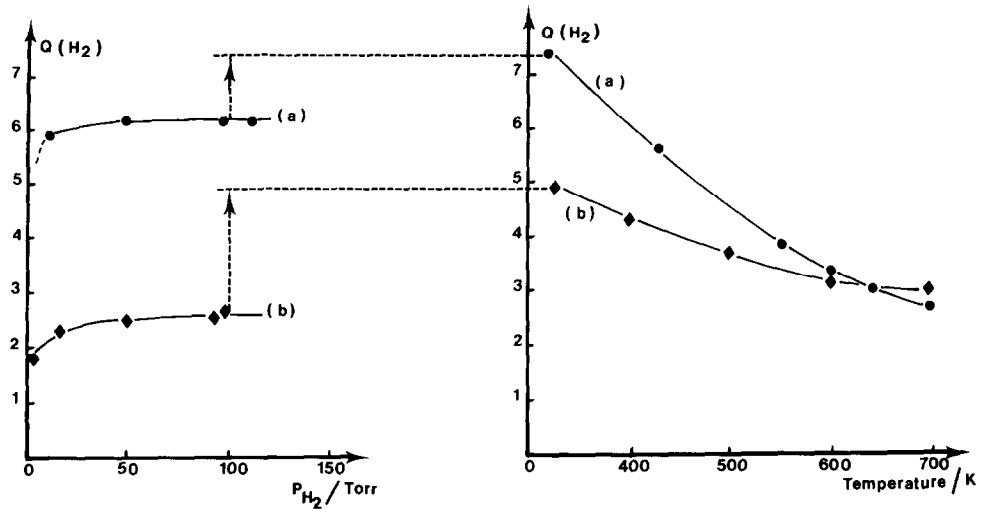

FIG. 3. I-H_2 adsorption isotherms at 300 K; (a) PtY,I; (b) PtMoY,III (the dashed arrows indicate the amount of H_2 taken up on heating from 300 to 573 K and cooling from 573 to 300 K). II-H_2 adsorption isobars under 100 Torr of H_2; (a) PtY,I; (b) PtMoY,III.

The H_2 adsorption isotherms at 300 K and the isobars under 100 Torr of H_2 corresponding to PtY,I and PtMoY,III are given in Fig. 3. In this set of experiments the isotherms and isobars were determined for PtY,I first, then $Mo(CO)_6$ vapor was adsorbed and decomposed *in situ* in the adsorption cell and after outgassing at 670 K the isotherms and isobars were determined for PtMoY,III. The amount $Q_2(H_2)$ is indicated by the dashed arrows.

The programmed thermodesorption curves of H_2 adsorbed on PtY,I and Pt MoY,III are given in Fig. 4. Curves 1a and 1b corresponding to the 300 K H_2 adsorption on PtY,I and PtMoY,III, respectively, are compared with curves 2a and 2b corresponding to the 573 K H_2 adsorption on the two samples. It is conspicuous that the H_2 adsorption at high temperature on PtMoY,III leads to a strongly held hydrogen form which gives a high temperature desorption peak.

The results from O_2 adsorption and H_2 titration are given in Table 3. On PtY,I the O_2 uptake ($Q(O_2)$) is two times smaller than $Q(H_2)$. On the other hand $Q(O_2)$ values on the PtMoY zeolite are larger than they should be if O_2 is adsorbed only on Pt; a fraction of the O_2 uptake is therefore consumed to oxidize the molybdenum. The ratio O/Mo was calculated by assuming that the Pt atoms adsorb two times less O_2 than H_2 as they do on PtY,I. The oxidation number of Mo species in PtMoY,III should be increased by 1 since 0.5 O atom is consumed per 1 Mo atom. The values of $T(H_2)$ indicate that the whole amount of O_2 taken up is titrated at 300 K by H_2 in the case of PtMoY,I and PtMoY,III. However, on Pt MoY,VI part of the O_2 taken up is not titrated, which indicates that the Mo species oxidized at 300 K by O_2 are not reduced at 300 K by H_2.

TABLE 3

O_2 Adsorption and H_2 Titration[a]

Sample	Pt/(Pt + Mo)	$Q_1(H_2)$[b]	$Q(O_2)$[c]	O/Mo[d]	$T(H_2)$[e]
PtY,I	1	6.1	3.4		
PtMoY,I	0.82	4.2	3.0	0.64	10.0
PtMoY,III	0.48	2.3	4.2	0.46	9.3
PtMoY,VI	0.04	0.08	1.9	0.30	0.25

[a] Amount of gases are given in cm^3 (NTP) g^{-1} of catalyst.
[b] See Table 2, amount of H_2 adsorbed at 300 K.
[c] $Q(O_2)$ uptake of O_2 at 300 K under 50 Torr of O_2 on outgassed catalyst.
[d] O/Mo ratio calculated from $Q(O_2)$ by assuming that the Pt atoms adsorb two times less O_2 than H_2.
[e] $T(H_2)$ uptake of H_2 at 300 K under 50 Torr on catalyst covered with O_2 at 300 K.

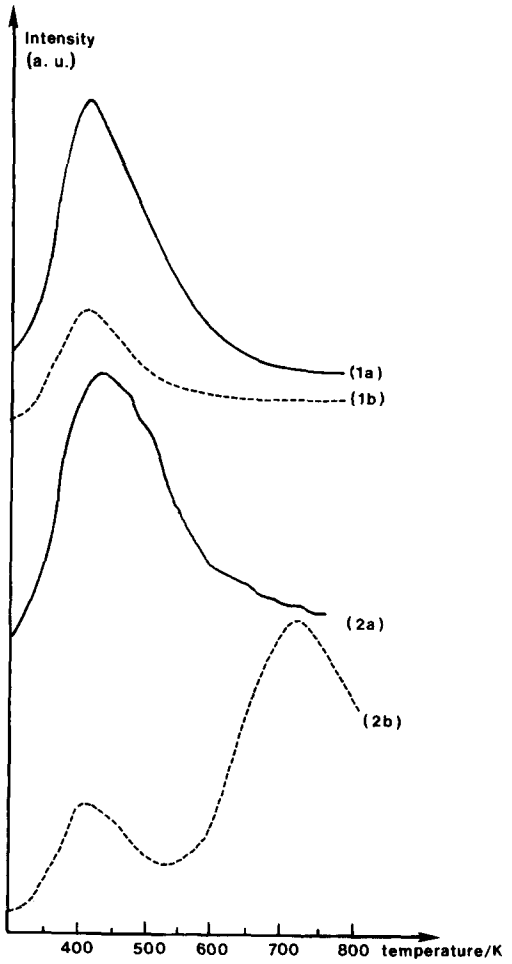

FIG. 4. Programmed thermodesorption curves of H_2. (1a) PtY,I, H_2 adsorbed at 300 K; (1b) PtMoY,III, H_2 adsorbed at 300 K; (2a) PtY,I, H_2 adsorbed at 573 K; (2b) PtMoY,III, H_2 adsorbed at 573 K.

3. *Absorption Edge Spectroscopy*

The PtY,I and PtMoY,III zeolites have been reduced and outgassed at 573 K, then the samples were contacted with 760 Torr of H_2 at 300 K and kept as such during the recording of the Pt L III edge spectroscopy data. The white line area was measured and compared to that of a platinum foil as previously described (*9*). The relative white line areas follow the sequence Pt : PtMoY, III : PtY,I = 1.0 : 1.0 : 1.3.

4. *Infrared Spectroscopy Study*

The zeolite wafers were treated in the ir cell at 573 K in vacuum–H_2–vacuum successively, then the spectra have been recorded after adsorbing CO under 50 Torr pressure at 300 K and after desorption at the same temperature. The zeolites were then heated at 573 K in O_2–vacuum–H_2–vacuum, successively, to clean the particle surface. Then NO was adsorbed at 50 Torr pressure at 300 K, and evacuated at the same temperature. The frequencies and optical densities of the CO and NO absorption bands are given in Table 4. Data corresponding to PtY,II zeolite whose acidity has been neutralized in 0.1 *N* NaOH solution (it was checked that the ν_{OH} bands vanished) and to Pt/Al_2O_3 and Pt/SiO_2 catalysts are given in comparison. The ir spectra of the zeolite samples in the CO and NO stretching frequency regions are given in Fig. 5. The optical densities of the ν_{CO} band at 2065–2090 cm^{-1} normalized at 1 for PtY,I are given in Fig. 2.

As in the previous investigations (*4*, *9*) the ir band at 2067–2090 cm^{-1} was attributed to CO linearly bonded to Pt atoms and those at 1795–1895 cm^{-1} were attributed to CO in bridging positions between Pt atoms.

5. *XPS Study*

Photoelectron emission can probe the atoms in the zeolite crystal within a 25- to 50-Å-thick layer. The intensity of the core level peaks of Pt $4f_{7/2}$ and Mo $3d_{5/2}$ have been compared to that of Si 2s in order to check the homogeneity of the metal atom distribution near the external surface. Table 5 gives the ratios of the intensity of the Pt and Mo peaks over that of the Si 2s line in comparison with the Pt/Si and Mo/Si ratios derived from the chemical composition of the zeolite bulk. Platinum is always homogeneously dispersed in the studied samples. On the contrary, incorporation of Mo atoms on the samples rich in Mo is partly heterogeneous since the XPS results show an enrichment in Mo of the outer layer. For samples with a low molybdenum content, addition of Mo is homogeneous, in agreement with the quasilinear decrease of both

TABLE 4

Frequencies and Optical Densities of ir Bands of CO and NO Adsorbed as Probe Molecules

Samples	Pt/(Pt + Mo)	ν_{CO}[a] (OD)	ν_{CO}[b] (OD)	ν_{NO}[c] (OD)
PtY,I	1	2090 (4.5)	1895 (0.8); 1845 (0.9); 1800 (0.4)	1835 (2.2)
PtMoY,I	0.82	2080 (2.4)	1865 (0.2)	1807 (1.11)
PtMoY,II	0.61	2072 (1.1)	1850 (very weak)	1810[b] (1.31) 1700
PtMoY,III	0.48	2067 (0.7)		1805[b] (0.72) 1700
PtY,II	1	2085	1890; 1840; 1800	
PtY,II + NaOH	1	2068	1890; 1840; 1795	
Pt/Al_2O_3	1	2080[d]	1850 (very weak)[d]	1815[f] (for 15-Å particle size)
Pt/SiO_2[e]	1	2070	1850 (very weak)	

[a] Stretching frequency of linearly bonded CO (frequencies are in cm^{-1} and OD is the optical density normalized at 0.1 g of PtY).

[b] Stretching frequency of bridging CO.

[c] Stretching frequency of linearly bonded NO.

[d] Ref. (*19*).

[e] Europt 1, Council of Europe Research Group in Catalysis, P. B. Wells, University of Hull, U.K., 1981.

[f] Ref. (*9*).

$Q_1(H_2)$ and the optical density of the ν_{CO} band at 2090–2067 cm^{-1} with the Pt/(Pt + Mo) ratio decreasing from 1 to 0.5 which is in favor of a quasihomogeneous dispersion of molybdenum.

The binding energies of the Pt $4f_{7/2}$ levels are given in Table 5 for various PtY and PtMoY zeolites rereduced *in situ* before XPS measurements. The XPS spectra in the region of the Mo 3d emission band are given in Fig. 6; the XPS spectrum of a Mo NaY zeolite and the binding energies of Mo^0, Mo^{4+}, and Mo^{5+} are inset for comparison.

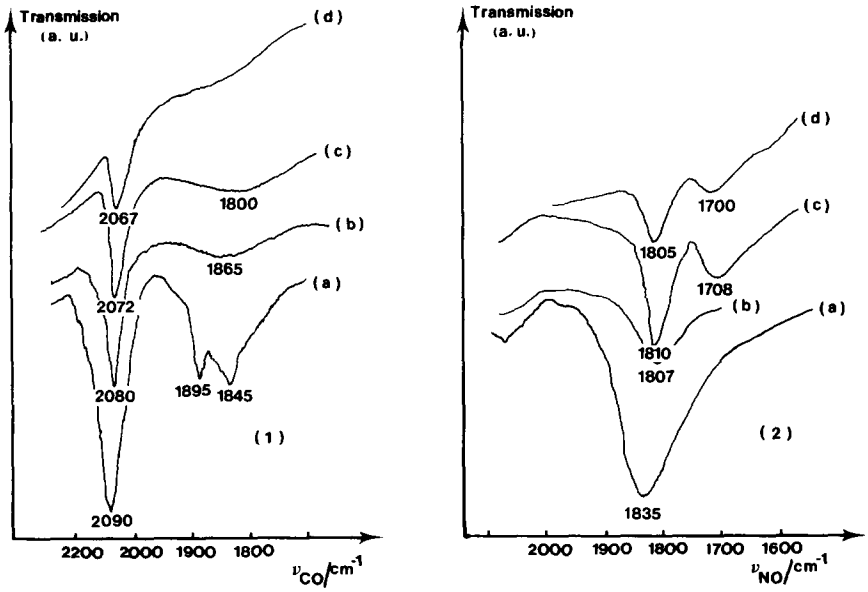

FIG. 5. Infrared spectra of CO and NO irreversibly adsorbed at 300 K; (a) PtY,I; (b) PtMoY,I; (c) PtMoY,II; (d) PtMoY,III.

TABLE 5

XPS Study of the Outer Layer Composition and Pt $4f_{7/2}$ Binding Energies

Samples	Pt/(Pt + Mo)[a]	Pt/Si[a]	Mo/Si[a]	Treatments[b]	(Pt $4f_{7/2}$)/(Si 2s)	(Mo 3d)/(Si 2s)	Binding energies Pt $4f_{7/2}$ (eV ± 0.3)
Bulk Pt[c]							71.5
PtY (10 Å)[c]				H_2, 573 K; vacuum, 573 K			72.2
PtMoY,I	0.82	0.05	0.01	H_2, 300 K; vacuum, 300 K	0.04	0.01	71.3
PtMoY,I	0.82	0.05	0.01	H_2, 573 K; 15 h	0.04	0.01	71.3
PtMoY,III	0.48	0.06	0.06	H_2, 573 K; 15 h	0.07	0.2	71.6
PtMoY,V	0.29	0.02	0.06	H_2, 300 K; vacuum, 573 K	0.03	0.3	71.5
PtMoY,V	0.29	0.02	0.06	H_2, 573 K; 15 h	0.03	0.3	71.5

[a] Ratio derived from the bulk chemical composition.
[b] *In situ* treatments before XPS measurements, maximum temperature 573 K, maximum H_2 pressure, 1 Torr.
[c] Védrine *et al.* (6).

The zeolites were treated in the ESCA apparatus at a maximum temperature of 573 K and under a maximum pressure of 1 Torr of H_2. These conditions are adequate to reduce the Pt atoms covered by O_2 but they are not stringent enough to reduce the Mo atoms reoxidized in air.

DISCUSSION

1. *Distribution of Pt and Mo in the Zeolite Crystals*

The distribution of the platinum in the zeolite framework is very homogeneous since (i) the CTEM investigation shows that the particles are uniformly scattered throughout the slabs cut across the zeolite crystals with an ultramicrotome; (ii) the X-ray spectrometer analysis with the STEM indicates a constant concentration of platinum from the edges to the center of the slabs; (iii) the ratio of the intensities of the emission bands of Pt $4f_{7/2}$ and Si 2s measured by XPS is similar to the ratio Pt/Si derived from bulk chemical analysis (Table 5).

The introduction of molybdenum into the zeolite porous framework has been successful in most samples since Mo was detected by the STEM analysis throughout the zeolite slabs. However, in MoNaY containing no platinum and in PtMoY,VI containing a small amount of platinum a fraction of the molybdenum coming from the $Mo(CO)_6$ decomposition was found in the form of large particles on the external surface of the zeolites. In the other PtMoY samples the concentration of Mo with respect to that of Pt varies from crystal to crystal and decreases from the outer layers to the core of a given slab; this is especially true in Mo-rich samples where the Pt/

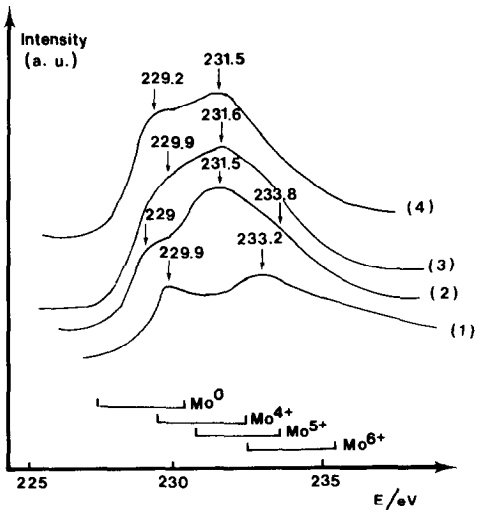

FIG. 6. XPS spectra of Mo 3d after *in situ* reduction under 0.1 Torr of H_2 and various temperatures and periods of time. (1) MoNaY, 573 K, 15 h; (2) PtMoY,V, 300 K, 2 h; (3) PtMoY,V, 573 K, 2 h; (4) PtMoY,V, 573 K, 15 h. These spectra are typically the addition of underlying spectra corresponding to different oxidation states.

(Pt + Mo) ratio is smaller than 0.5. This is corroborated by the XPS study (Table 5). In PtMoY,I (Pt/(Pt + Mo) = 0.82) there is a good agreement between the Mo/Si ratios derived from the bulk composition and the Mo 3d/Si 2s ratio indicating no surface enrichment in molybdenum, whereas the two sets of ratio differ markedly in PtMoY,V proving that larger amounts of $Mo(CO)_6$ were adsorbed and decomposed in the outer layers than in the zeolite bulk.

It appears, therefore, that the presence of platinum particles which are uniformly distributed favors the adsorption of $Mo(CO)_6$ and the homogeneity of the final material. In a previous study (*10*) dealing with $Mo(CO)_6$ adsorption and decomposition in a HY zeolite loaded with 8 $Mo(CO)_6$ molecules per unit cell (one per supercage) it was shown that the $Mo(CO)_6$ molecules were adsorbed near the center of the 12-membered oxygen-ring interacting with the O_1H hydroxyl groups of the framework, and that the molybdenum atoms freed by decomposition were still located in the vicinity of these sites. It can be inferred that protons or platinum atoms serve as anchoring sites for the $Mo(CO)_6$ molecules which are therefore more readily adsorbed and homogeneously distributed than in the Mo-NaY or in the Pt-poor PtMoY zeolite. This is supported by the fact that the sublimation of the $Mo(CO)_6$ crystals during the preparation of the PtMoY zeolite is much more rapid in the case of HY or Pt-rich zeolites.

These results led us to conclude that in the PtMoY samples where Pt/(Pt + Mo) <0.5 there is a sizable fraction of the molybdenum which is not in the vicinity of the Pt particles. On the other hand, in all the samples, it is highly probable that all the Pt particles are interacting with molybdenum.

2. *Size of the Particles*

The size distribution of the platinum particles found in the PtY zeolites by CTEM investigation is in good agreement with all the previous work showing that 1 ± 0.3-nm particles are formed when the Pt-exchanged Y-zeolites are treated under flowing O_2 and reduced by hydrogen at 573 K, provided the oxygen treatment is performed under well-defined conditions (slow temperature increase, high O_2 flux, small zeolite batch).

The size distribution obtained after $Mo(CO)_6$ adsorption and decomposition is always shifted upward. Thus Fig. 1 indicates that the average particle diameter increases by 0.1 nm in the case of the PtY,I→ PtMoY,III preparation. This increase is small but it can be expected from a simple model calculation. Thus if on a 19-atom c.f.c. particle (octahedron with 3 Pt atoms along the edge) whose maximum dimension is 1.06 nm, 24 Mo atoms are added following the rules of the c.f.c. close packed arrangement the maximum dimension of the resulting particle is only 1.24 nm.

We are unable to specify with certainty the number of atoms in the platinum particles (since several models containing different number of atoms are compatible with a given size and there is a size distribution between 6 and 13 Å) or the number of Mo atoms which could be added. However, the particle size increase cannot be due to a sintering of the Pt particles during PtMoY catalyst preparation since these particles are stable up to 1073 K (2); therefore it must be due to the addition of molybdenum atoms on the platinum particles.

3. *Adsorption Properties at 300 K*

As far as H_2 chemisorption is concerned, the platinum in PtY,I is 100% dispersed (if we assume a H/Pt = 1 stoichiometry) since the H/Pt ratio is 1 (Table 2). This is in agreement with previous findings (*2*) and with the 1 ± 0.3 nm size of these particles measured by CTEM. We can assume that all the Pt atoms are accessible to hydrogen chemisorption. The striking fact is that on progressive Mo additions on the zeolites the H_2 chemisorption is suppressed (Table 2). If we except PtMo,VI where a large fraction of the molybdenum is not interact-

ing with platinum, the decrease of the amount of chemisorbed hydrogen is almost linear (Fig. 2). Since the CTEM study indicates that there is only a small expansion of particle size, the decrease in the amount of chemisorbed H_2 cannot be due to a sintering effect.

A similar reduction of CO chemisorption has been observed by ir spectroscopy. The amount of chemisorbed CO monitored by the optical density of the ν_{CO} band at 2067–2090 cm^{-1} decreases almost linearly with Pt/(Pt + Mo) (Table 4, Fig. 2) and the negative slope of the curve is not much different from that of the H_2 uptake. Nevertheless, the chemisorption of CO on Pt is more inhibited by Mo than the H_2 chemisorption. Two explanations can be tentatively advanced: (i) the hindrance effect and (ii) the larger accessibility of H_2 compared to CO for Pt atoms. The optical densities of the ν_{CO} band at 1795–1895 cm^{-1} decrease even more rapidly with Mo addition in agreement with the fact that the number of ensembles of 2–3 Pt atoms available for CO in a bridging position decreases more rapidly than the number of masked Pt atoms. Finally, the optical density of the ν_{NO} band at 1805–1835 cm^{-1} also diminishes when Mo is added onto the platinum particles.

The molybdenum species formed in the zeolite do not adsorb hydrogen at 300 K, in contrast with Mo metal which is capable of chemisorbing hydrogen in these conditions. It is probable that the Mo species are not zero valent; this point will be confirmed in later sections. On the other hand, the Mo species adsorb oxygen, since the O_2 uptake at 300 K is larger than it should be if the Pt atoms were the sole adsorption sites (Table 3). This uptake probably corresponds to an oxidation of the molybdenum which is more marked on PtMoY,I where most of the Mo species interact with the Pt particles than on PtMoY,VI. Accordingly, this O_2 uptake can be titrated by H_2 at 300 K on PtMoY,I but only a small part is titrated on PtMoY,VI; the presence of Pt seems therefore necessary to reduce the oxygen atom fixed on molybdenum at 300 K.

Finally, the thermodesorption study of the H_2 chemisorbed at 300 K (Fig. 4) shows that the hydrogen adsorbed on PtY,I (curve 1a) and on PtMoY,III (curve 1b) desorbs at the same temperature, which indicates that H_2 is adsorbed on the same type of site (i.e., Pt atoms) and with the same strength whether Mo is present or not.

4. Adsorption Properties at Higher Temperatures

The PtY and PtMoY zeolites adsorb an additional amount of hydrogen ΔQ when they are heated up to 573 K and cooled to 300 K under 50 Torr of H_2 pressure (Table 2, Fig. 3). This uptake is not involved in a reduction process since it can be outgassed under vacuum at 673 K ($Q_2(H_2) = D_2(H_2)$ in Table 2). The total amount of H_2 adsorbed ($Q_2(H_2)$) decreases upon Mo loading, so the H_2 chemisorption at high temperature is also blocked by molybdenum as in the case of the H_2 chemisorption at 300 K.

The PtY zeolites adsorb less hydrogen at high temperature than the PtMoY zeolite; this is conspicuous in Fig. 3. Surprisingly, ΔQ cannot be correlated with the Pt or the Mo content but it does not vary much with the total atomic concentration in Pt and Mo (Table 2, column 9). The thermodesorption study of H_2 adsorbed at 573 K shows that the PtMoY,III zeolite exhibits two desorption peaks (Fig. 4, curve 2b) whereas only one peak is observed on the desorption curve of PtY,I (curve 2a). This high-temperature desorption peak corresponds to a form of hydrogen more strongly held on the metal phase. Consistently the isobar of H_2 adsorption on PtMoY,III shows that 63% of the chemisorbed H_2 remains attached to the surface at 673 K compared to only 36% on PtY,I. In spite of the fact that PtMoY,III adsorbs far less H_2 than PtY,I, the former sample retains more chemisorbed H_2 than the latter at 673 K, which suggests that the H_2 chemisorbed at high temperature is more strongly held than that adsorbed at

300 K. This form of hydrogen could be similar to that reported by one of us (*11*) which was attributed to H atom bridged between a surface Pt atom and a framework oxygen anion. Under the present conditions this hydrogen form could be in a bridging position between the Mo species and the oxygen anions.

5. Electronic Structure of Platinum

The X-ray absorption spectroscopy at the Pt L III edge can be used to probe the charge density on metal atoms, at least on a relative basis. Previous work has shown that a reliable comparison of the electron deficiency of platinum can be obtained by measuring the so-called white line area in a series of PtY zeolites where only the particle environment was allowed to change (*8*). The larger the Pt L III white line area, the larger the number of unoccupied states in the 5d and 6s band of platinum. The relative white line areas Pt metal : PtMoY,III : PtY,I = 1.0 : 1.0 : 1.3 indicates that the electron deficiency of platinum follows the sequence PtY,I > PtMoY,III = Pt metal = 0. The electron-deficient or electrophilic character (e.c.) of platinum in PtY zeolite has been discussed previously (*4, 8, 12, 13*). It was attributed mostly to an electron transfer from the metal particles to the electron acceptor sites of the support. The interesting point is that the addition of Mo on the zeolite suppresses the e.c. of the platinum particles.

The XPS study confirms these findings since the positive shift (+0.7 eV) of the Pt $4f_{7/2}$ binding energies in PtY zeolite with respect to Pt metal (*6*) which was indicative of platinum electron deficiency in the 1-nm particles encaged in Y-zeolite, disappears entirely in PtMoY,I, PtMoY,III, and Pt MoY,V. Therefore, the platinum particles have lost their e.c. and as far as XPS is concerned, they behave like bulk metal even when comparatively low amounts of Mo are loaded (PtMoY,I).

The ir study of the electronic properties of platinum using CO and NO as probe molecules leads to the same conclusion. In PtY,I the ν_{CO} frequency of linearly adsorbed CO on Pt at 2090 cm^{-1} is shifted by 20 cm^{-1} with respect to Pt/SiO_2 and 10 cm^{-1} with respect to Pt/Al_2O_3 (Table 4). This was attributed to the e.c. of Pt particles in PtY zeolites (*10*) which reduces the extent of back-donation of *d* electrons from the metal to the π^* antibonding orbital of the CO molecule, producing a decrease of the force constant of the C—O bond and a shift of the ν_{CO} frequency toward lower wavenumbers. The e.c. character is mainly due to an electron transfer from the metal to the support since it disappears when the zeolite acidity is neutralized by NaOH solution. Thus ν_{CO} decreases from 2085 cm^{-1} in PtY,II to 2068 cm^{-1} in PtY,II + NaOH, while the Brønsted acidity monitored by the ν_{OH} bands at 3650 and 3540 cm^{-1} vanishes. The e.c. of platinum in PtY,I is also progressively suppressed when Mo is added onto the zeolite since the ν_{CO} frequency decreases from 2090 to 2067 cm^{-1}.

Infrared results of NO adsorbed on surfaces have to be examined cautiously, since the nature of the surface can be modified by NO which is very reactive in comparison with CO. For instance, NO contacted with NaY Pd zeolites is able to produce at room temperature an oxidative dissolution of 20-Å palladium particles leading to nitrosyl complexes of Pd(II) ions anchored to the porous lattice (*14*). In this reaction, the formation of weakly adsorbed N_2O has been evidenced. For PtMoY samples, it has been checked that neither N_2O nor N_2 is present in the gas phase. Thus it can be assumed that no surface reactions of NO with the catalyst occur. The ν_{NO} frequency of NO adsorbed on the particles is, as for ν_{CO}, shifted down from 1835 cm^{-1} in PtY,I to 1805 cm^{-1} in PtMoY,III. The additional band at about 1700 cm^{-1} detected in presence of Mo has been attributed to the nitrosyl complex of molybdenum. Since there is no change in the Pt particle size, the shift observed in the ν_{NO} frequency must be correlated with the changes of the electrophilic

character of surface Pt atoms due to Mo additives. It can be noticed that in the case of NO the downward frequency shift is already completed (-30 cm^{-1}) in PtMoY,I containing a comparatively small amount of Mo; this is in agreement with XPS results showing that the +0.7 eV shift of the binding energies observed in PtY,I is suppressed in PtMoY,I. On the other hand, when CO is used as probe molecule the shift of ν_{CO} is progressive and is completed in PtMoY,III, i.e., when there are as many Mo atoms as Pt atoms.

To sum up, three independent methods demonstrate that the Mo addition on the zeolite produces an increase of the density of charge on the metal so that the platinum initially electron deficient behaves like bulk Pt in PtMoY zeolite. Three redox mechanisms can account for the modification of electronic structure; (i) there is a charge transfer from the Mo atoms to the electron acceptor sites of the zeolite which weakens or suppresses the electron transfer from the Pt atoms so that the Pt particles are no longer electrophilic; (ii) the Mo atoms added on the particles interact directly with the Pt atoms and because of the larger oxidation potential of Mo a charge transfer such as $Mo^0 + Pt^{\delta+} \rightarrow Mo^{\delta+} + Pt^0$ suppresses the e.c. of platinum; and (iii) the Pt atoms covered by Mo atoms are shielded from the electron acceptor sites and lose their e.c. Since the shift of the XPS binding energies and of the ν_{NO} frequency occurs at low loading, i.e., when most of the Mo atoms are fixed on the Pt particles, hypotheses ii and iii are more likely than hypothesis i.

6. *Electronic Structure of Molybdenum*

The valence state of the molybdenum in freshly prepared PtMoY zeolites is ill-defined since the electronic structure was studied by XPS after the samples had been contacted with air and the reduction conditions in the ESCA apparatus were not stringent enough to be sure that the Mo atoms oxidized in air have been rereduced to their initial level. Moreover, the XPS study was carried out on the PtMoY,V zeolite which contains many Mo atoms not bonded to Pt atoms (Section 1), which are liable to be in a higher oxidation state because of their interaction with the zeolite protons (vide infra) and which are more difficult to reduce because they are not in the vicinity of platinum. These atoms in the outer layers of the zeolite are actually those which are probed by XPS. Indeed, the results given in Figure 6 show that the XPS data on PtMoY,V reduced for 15 h at 573 K (curve 4) correspond to a mixture of Mo^{IV}, Mo^{V}, and Mo^{VI}. Higher valence states are observed on MoNaY (curve 1) and on PtMoY,V reduced for a shorter period of time or at a lower temperature (curves 2–3).

There are several valence states because of the heterogeneous distribution of Mo with respect to Pt, particularly in highly Mo-loaded samples where there is a surface enrichment in Mo. As shown in a previous study (*10*), the $Mo(CO)_6$ molecules adsorbed in Y-zeolites interact with the O_1H hydroxyl groups on the 12-membered oxygen ring and the thermal decomposition is followed by a redox reaction of the Mo^0 atoms with the zeolite protons:

$$Mo^0 + xH^+ \rightarrow x/2\ H_2 + Mo^{x+}$$

The hydrogen evolved from the zeolite was detected by mass spectrometry and the Mo^V species was characterized by EPR and uv spectroscopies. A similar oxidation mechanism of Mo produced by $Mo(CO)_6$ decomposition was described by Brenner and Burwell in the case of Pt/Al_2O_3 (*15*). Therefore it is highly probable that the $Mo(CO)_6$ decomposed in the zeolite cages free from platinum is also oxidized to Mo^{IV}–Mo^{VI} species as detected by XPS. On the other hand, the Mo atoms fixed in the cages containing Pt atoms should be in a lower valence state because they are formed in the presence of H atoms dissociated on platinum. However, they are not in a zero valent state even under more stringent reduction conditions such as those ap-

plied before H_2 adsorption studies (673 K under 600 Torr of H_2) since they do not adsorb hydrogen whereas Mo metal does. In fact even if these atoms are formally reduced or kept at a zero valent state during the catalyst preparation these atoms should transfer electrons toward the acceptor sites of the support and even to the Pt atoms since the latter lose their e.c. as discussed in the previous section.

To sum up, it can be concluded that despite the uncertainty in the XPS measurement of the valence state of molybdenum there are two kinds of Mo species after $Mo(CO)_6$ decomposition according to whether these atoms are interacting with the Pt particles or not. In the first case they are in a low-valence state interacting both with the Pt atoms and with the framework oxygen atoms, while in the second case they are in a high oxidation state and cannot be reduced under the normal conditions of reduction.

7. State of the Bimetallic Phase in PtMoY

When the $Mo(CO)_6$ molecules enter the porous zeolite framework they migrate first toward the zeolite supercages where 1-nm Pt particles are trapped and they remain there after decomposition since the properties of the platinum particles are modified even when small amounts of molybdenum are present. The most striking change which occurs is that platinum atoms progressively lose their ability to chemisorb H_2, CO, or NO when Mo is loaded. This can be explained by two effects: (i) the chemisorptive properties of platinum are inhibited because its electronic structure is perturbed by the molybdenum atoms; and (ii) the Pt atoms are physically masked by the Mo atoms deposited on the surface of the Pt particles. Hypothesis (ii) can be upheld for a number of reasons. The sizes of the particles increase upon Mo loading which indicates that Mo atoms are added on the surface. The amount of H_2 adsorbed decreases approximately as that of CO whereas one would have expected a different dependence with Mo loading if the inhibition was due to a change in electronic properties. Also the strength of H_2 adsorption would also be smaller whereas the thermodesorption study of H_2 coadsorbed at 300 K shows that the hydrogen atoms are as strongly held on PtMoY,III as they are on PtY,I. Finally Mo addition suppresses the e.c. of platinum so that it behaves like bulk Pt with respect to the three methods used; this could not account for the inhibition of the chemisorptive properties.

The bimetallic phase in the PtMoY zeolites can therefore be described as 1.2 ± 0.3-nm particles formed by a core of zero valent platinum on which Mo atoms are progressively added following the rule of the f.c.c. close packing arrangement. This addition leaves less and less Pt atoms accessible to the adsorbates. Thus in PtMoY, III, where there are as many Mo atoms as Pt atoms, one-half of the Pt atoms remain accessible to hydrogen, only one-third are still available for chemisorption of linearly bonded CO, but none remains available for adsorption of CO in bridging positions.

This model bears some relationships with that proposed by Yermakov *et al.* (*1, 16*) for $PtMo/SiO_2$ catalysts. In both cases the bimetallic phase is formed by very small clusters where the Mo atoms are in a low-valence state. The differences arise mainly from the mode of preparation. In the present work the clusters are built by addition of Mo atoms to a core formed by 1-nm Pt particles, whereas in the $PtMo/SiO_2$ system the molybdenum was reduced first and the platinum atoms were added onto a core formed by one or several Mo low-valent species. The main difference is the valence state of platinum which was claimed to be electron deficient in $PtMo/SiO_2$ (*16, 17*) as a result of electron transfer toward the Mo species whereas in the present case the platinum is without any doubt electron deficient before Mo addition and strictly zero valent after, probably because the Mo species added shield the underlying Pt atoms from the electron acceptor sites of the zeo-

lite which now interact with the Mo species. Here again the different valence state of platinum in the two systems can be explained by the two different preparative modes and by the different nature of the supports.

In Part II of this work (*17*) it will be shown how the model described above for the bimetallic phase in PtMoY zeolites can account for the very original behavior of these catalysts in hydrocarbon conversion reactions.

ACKNOWLEDGMENTS

We thank Mrs. C. Leclerc and I. Mutin for studying the catalysts by CTEM and STEM. The Institut Français du Petrole, and MM. Freud and Dexpert are gratefully acknowledged for making the STEM available for that study.

REFERENCES

1. Yermakov, Yu. I., and Kuznetsov, B. N., *J. Mol. Catal.* **9,** 13 (1980).
2. Gallezot, P., Alarcon-Diaz, A., Dalmon, J.-A., Renouprez, A. J., and Imelik, B., *J. Catal.* **39,** 334 (1975).
3. Gallezot, P., Mutin, I., Dalmai-Imelik, G., and Imelik, B., *J. Microsc. Spectrosc. Electron.* **1,** 1 (1976).
4. Gallezot, P., Datka, J., Massardier, J., Primet, M., and Imelik, B., Proc. Int. Congr. Catalysis 6th, (London 1976), p. 696. Chemical Society, London, 1977.
5. Gallezot, P., Bienenstock, A., and Boudart, M., *Nouv. J. Chim.* **2,** 263 (1978).
6. Védrine, J. C., Dufaux, M., Naccache, C., and Imelik, B., *J. Chem. Soc. Faraday I* **74,** 440 (1978).
7. Gallezot, P., *Catal. Rev.-Sci. Eng.* **20,** 121 (1979).
8. Gallezot, P., Weber, R., Dalla Betta, R. A., and Boudart, M., *Z. Naturforsch.* **34A,** 40 (1979).
9. Primet, M., Basset, J.-M., Garbowski, E., and Mathieu, M. V., *J. Amer. Chem. Soc.* **97,** 3655, 1975.
10. Gallezot, P., Coudurier, G., Primet, M., and Imelik, B., *in* "Molecular Sieves II" (J. R. Katzer, Ed.), p. 144. American Chemical Society, Washington, D.C., 1977.
11. Candy, J.-P., Fouilloux, P., and Renouprez, A. J., *J. C. S. Faraday I* **76,** 616 (1980).
12. Dalla Betta, R. A., and Boudart, M., Proc. Int. Congr. Catalysis 5th, (Florida 1972), p. 1329. North Holland, Amsterdam, 1973.
13. Tri, T. M., Massardier, J., Gallezot, P., and Imelik, B., Proc. Int. Congr. Catalysis 7th, (Tokyo 1980), p. 266. Elsevier, Amsterdam, 1981.
14. Che, M., Dutel, J. F., Gallezot, P., and Primet, M., *J. Phys. Chem.* **80,** 2371 (1976).
15. Brenner, A., and Burwell, R. L., *J. Catal.* **52,** 353 (1978).
16. Yermakov, Yu. I., Kuznetsov, B. N., and Ryndin, Yu. A., *J. Catal.* **42,** 73 (1976).
17. Ioffe, M. S., Shalga, Yu. M., Ryndin, Yu. A., Kuznetsov, B. N., Startsev, A. N., Borodko, Yu. G., and Yermakov, Yu. I., *React. Kinet. Catal. Lett.* **4,** 229 (1976).
18. Tri, T. M., Gallezot, P., Massardier, J., and Imelik, B., in preparation.
19. Primet, M., Basset, J.-M., Mathieu, M. V., and Prettre, M., *J. Catal.* **28,** 368 (1973).